

Curvature radius and Kerr black hole shadow

Shao-Wen Wei^{1,2}, Yuan-Chuan Zou^{3,4}, Yu-Xiao Liu¹, Robert B. Mann²

¹Institute of Theoretical Physics & Research Center of Gravitation, Lanzhou University, Lanzhou 730000, People's Republic of China

²Department of Physics and Astronomy, University of Waterloo, Waterloo, Ontario, Canada, N2L 3G1

³School of Physics, Huazhong University of Science and Technology, Wuhan 430074, People's Republic of China

⁴Perimeter Institute, 31 Caroline St., Waterloo, Ontario, N2L 2Y5, Canada

E-mail: weishw@lzu.edu.cn, zouyc@hust.edu.cn, liuyx@lzu.edu.cn, rbmann@uwaterloo.ca

Abstract. We consider applications of the curvature radius of a Kerr black hole shadow and propose three new approaches to simultaneously determine the black hole spin and inclination angle of the observer. The first one uses only two symmetric characteristic points, i.e., the top and the bottom points of the shadow, and is the smallest amount of data employed to extract information about spin and inclination angle amongst all current treatments. The second approach shows that only measuring the curvature radius at the characteristic points can also yield the black hole spin and the inclination angle. The observables used in the third approach have large changes to the spin and the inclination angle, which may give us a more accurate way to determine these parameters. Moreover, by modeling the supermassive black hole M87* with a Kerr black hole, we calculate the angular size for these curvature radii of the shadow. Some novel properties are found and analyzed. The results may shine new light on the relationship between the curvature radius and the black hole shadow, and provide several different approaches to test the nature of the black hole through the shadow.

Keywords: Black holes, shadow, null geodesics

Contents

1	Introduction	1
2	Null geodesics and shadow	2
3	Determining spin and inclination angle	4
3.1	Approach I	4
3.2	Approach II	8
3.3	Approach III	9
4	Application to M87*	10
5	Conclusions and discussions	11

1 Introduction

Very recently, the Event Horizon Telescope (EHT) has showcased the first image of the supermassive black hole M87* [1–3]. This fruitful outcome reveals a fine structure near the black hole horizon. The photon ring and shadow have been clearly observed, which provides us with a good opportunity to test general relativity in the regime of strong gravity. Combined with upcoming telescope surveys, such as the Next Generation Very Large Array [4] and the Thirty Meter Telescope [5], more high-resolution observations will yield important new information about strong gravity.

A black hole shadow is a two dimensional dark zone in the celestial sphere caused by the strong gravity of the black hole. It was first studied by Synge in 1966 for a Schwarzschild black hole [6]. Later, a formula for the angular radius for the shadow was given by Luminet [7]. In general, the shadow cast by a non-rotating black hole is a standard circle, whereas for a rotating black hole the shadow will be elongated in the direction of the rotating axis due to spacetime dragging effects [8, 9]. In order to match astronomical observations, Hioki and Maeda [10] proposed two observables based on the characteristic points on the boundary of the Kerr shadow. One approximately describes the size of the shadow, and another describes the deformation of its shape from a reference circle. This approach has been extended to other black holes [11–42], and a coordinate-independent study of the shadow by making use of Legendre polynomials has been carried out [43].

Information about the properties of a black hole is contained on the boundary of its shadow. So if the boundary curve is uniquely determined, we can extract this information from it. Motivated by this idea we recently introduced a new concept, the local curvature radius [39], from the viewpoint of differential geometry. For each fixed black hole spin and inclination angle of the observer, we found there exists one minimum and one maximum of the curvature radius upon taking the symmetry of the black hole shadow into account. Employing this property we showed that both the spin and the inclination angle can be uniquely determined.

We further extended our application of the local curvature radius to construct a topological quantity [39] associated with the shadow. The value of this quantity is unity for an arbitrary Kerr black hole, but smaller than one for a naked singularity. Using this quantity,

we can therefore distinguish a black hole from a naked singularity. It can be used to measure the topological structure for the multi-shadows in some special spacetimes.

The aim of this paper is to further explore applications of the local curvature radius. Noting that the maximum curvature always occurs at the left point of the shadow whereas the corresponding point of the minimum curvature varies with the black hole parameters [39], we focus on how to extract black hole parameters from this information. Rather than measuring the curvature radius at every point on the shadow boundary, we can exploit the symmetry of the shadow to obtain its characteristic points, making use of a detailed study we have previously carried out [44]. In the Kerr spacetime, these points have analytical coordinates for the equatorial observer, and away from the equatorial plane these points are also very easy to work out.

It is therefore natural to combine the curvature radius and characteristic points to determine the black hole parameters. Three novel approaches are presented in this paper. These results demonstrate that the local curvature radius is a very useful tool in the study of black hole shadows. We apply our results on the curvature radius to the supermassive black hole M87*.

Our paper is organized as follows. In Sec. 2, we briefly review the null geodesics and shadow for the Kerr black hole. Then the curvature radius is introduced. In Sec. 3, we show how to determine the black hole spin and the inclination angle of the observer by making use the curvature radius. Three approaches are proposed for different purposes. We then consider the supermassive M87* black hole in Sec. 4. Finally, the conclusions and discussions are presented in Sec. 5.

2 Null geodesics and shadow

Here we provide a brief review of the null geodesics and shapes of the shadow in a Kerr spacetime.

In Boyer-Lindquist coordinates, the line element in a Kerr spacetime is

$$ds^2 = - \left(1 - \frac{2Mr}{\rho^2} \right) dt^2 + \frac{\rho^2}{\Delta} dr^2 + \rho^2 d\theta^2 - \frac{4Mra \sin^2 \theta}{\rho^2} dt d\phi + \frac{((r^2 + a^2)^2 - \Delta a^2 \sin^2 \theta) \sin^2 \theta}{\rho^2} d\phi^2, \quad (2.1)$$

where the metric functions are

$$\Delta = r^2 - 2Mr + a^2, \quad \rho^2 = r^2 + a^2 \cos^2 \theta. \quad (2.2)$$

The parameters M and a are, respectively, the black hole mass and spin. The horizons in a Kerr spacetime can be obtained by solving $\Delta(r) = 0$, which are located at

$$r_{\pm} = M \pm \sqrt{M^2 - a^2}. \quad (2.3)$$

There are two horizons for $|a| < M$ and one horizon for $|a| = M$; no horizon exists for $|a| > M$, which corresponds to a naked singularity.

The null geodesics in the Kerr spacetime are given by the solutions to the equations

$$\rho^2 \frac{dt}{d\lambda} = a(l - aE \sin^2 \theta) + \frac{r^2 + a^2}{\Delta} (E(r^2 + a^2) - al), \quad (2.4)$$

$$\rho^2 \frac{dr}{d\lambda} = \sqrt{\mathfrak{R}}, \quad (2.5)$$

$$\rho^2 \frac{d\theta}{d\lambda} = \sqrt{\Theta}, \quad (2.6)$$

$$\rho^2 \frac{d\phi}{d\lambda} = (l \csc^2 \theta - aE) + \frac{a}{\Delta} (E(r^2 + a^2) - al), \quad (2.7)$$

where λ is the affine parameter. The functions \mathfrak{R} and Θ are given by

$$\mathfrak{R} = (a^2 E - al + Er^2)^2 - \Delta (\mathcal{Q} + (l - aE)^2), \quad (2.8)$$

$$\Theta = \mathcal{Q} - (l \csc \theta - aE \sin \theta)^2 + (l - aE)^2. \quad (2.9)$$

Here the conserved quantities l and E are the angular momentum and energy of the test particle, which are related with the Killing vector fields ∂_ϕ and ∂_t , respectively. The conserved Carter constant \mathcal{Q} is related to the Killing-Yano tensor field in the Kerr spacetime [45, 46]. Moreover, one can introduce two new parameters ξ and η

$$\xi = \frac{l}{E}, \quad \eta = \frac{\mathcal{Q}}{E^2}. \quad (2.10)$$

By making use of the null geodesics, we can obtain the two celestial coordinates α and β , which are used to describe the shape of the shadow that an observer seen in the sky. For an observer of the inclination angle θ_0 , the celestial coordinates are given by

$$\alpha = -\xi \csc \theta_0, \quad (2.11)$$

$$\beta = \pm \sqrt{\eta + a^2 \cos^2 \theta_0 - \xi^2 \cot^2 \theta_0}. \quad (2.12)$$

On the boundary, the parameters ξ and η are given by [47]

$$\xi = \frac{(3M - r_0)r_0^2 - a^2(M + r_0)}{a(r_0 - M)}, \quad (2.13)$$

$$\eta = \frac{r_0^3(4a^2M - r_0(3M - r_0)^2)}{a^2(r_0 - M)^2}. \quad (2.14)$$

where r_0 varies between the light ring radii of direct and retrograde photons along the boundary of the shadow. This also provides us with a parametrization of the form of the shadow, and based on it, some analytic results can be obtained Ref. [44]. For convenience, we show the shapes of the shadow for the black hole in Fig. 1 with spin $a/M = 0.98$, and inclination angle $\theta_0 = \frac{\pi}{2}, \frac{\pi}{3}, \frac{\pi}{4}$, and $\frac{\pi}{6}$ from right to left. In order to study them, we introduced a new quantity, the curvature radius R [39]. From the viewpoint of differential geometry, if we measure the curvature radius at each point of the boundary, the shadow will be uniquely determined, and then we can exactly read out the black hole parameters in a given spacetime, or to distinguish different gravity theories via the structure of the shadow.

We now briefly review how to calculate the local curvature radius [39]. From Eqs. (2.11) and (2.12), one can find that the celestial coordinates (α, β) for each point on the boundary of the shadow are parametrized by r_0 . Thus each value of r_0 corresponds to one

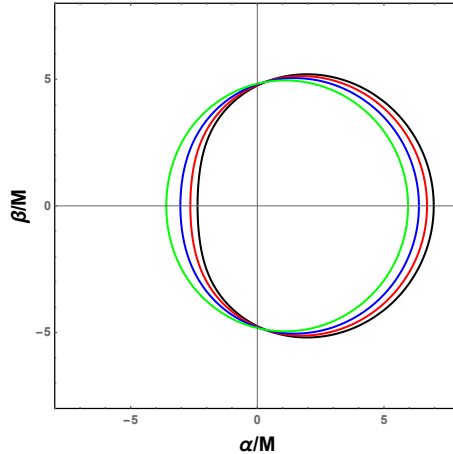


Figure 1. Shapes of the shadow in Kerr spacetime for $a/M = 0.98$ with the inclination angle $\theta_0 = \frac{\pi}{2}, \frac{\pi}{3}, \frac{\pi}{4},$ and $\frac{\pi}{6}$ from right to left.

point. In order to obtain the curvature radius, we consider three values of r_0 , i.e., $r_0 - \epsilon$, r_0 , and $r_0 + \epsilon$, yielding three points on the boundary, $(\alpha(r_0 - \epsilon), \beta(r_0 - \epsilon))$, $(\alpha(r_0), \beta(r_0))$, and $(\alpha(r_0 + \epsilon), \beta(r_0 + \epsilon))$ – from these we can uniquely plot a circle of radius $R(r_0, \epsilon)$. In the limit $\epsilon \rightarrow 0$, these three points approach the same point, and $R(r_0, \epsilon) \rightarrow R(r_0)$, which is just the curvature radius of the point $(\alpha(r_0), \beta(r_0))$. Adopting this method, we obtained the curvature radius for the Kerr black hole shadow, which reads [39]

$$R = \frac{64M^{1/2}(r_0^3 - a^2r_0 \cos^2 \theta_0)^{3/2} [r_0(r_0^2 - 3Mr_0 + 3M^2) - a^2M^2]}{(r_0 - M)^3 [3(8r_0^4 - a^4 - 8a^2r_0^2) - 4a^2(6r_0^2 + a^2) \cos(2\theta_0) - a^4 \cos(4\theta_0)]}. \quad (2.15)$$

Alternatively, we can parametrize R with the length parameter λ of the shadow. From this we proposed [39] a topological quantity $\delta = \int \frac{d\lambda}{R(\lambda)} + \sum_i \theta_i$ to measure the topological structure of the shadow. It can also be used to distinguish a shadow cast by a black hole from that of a naked singularity. In fact, this intrinsic curvature radius is critical for testing the black hole parameter through the shadow, and we will show it in the next section.

3 Determining spin and inclination angle

In this section, we show how to determine the spin a and inclination angle θ_0 for the Kerr black hole by making use of the curvature radius.

3.1 Approach I

Generally, there are two ways to test the black hole parameters and the viewing angle of the observer. The first one is that we can completely determine every point on the boundary of the shadow, and then fit the theoretical model. Thus we can find out the best values for the black hole parameters in the expected spacetime. This method can also be used to determine the possible modified theory. As shown above the shadow can be uniquely described by the curvature radius (2.15). However, this task is extremely hard because there are so many points on the boundary of the shadow. In order to make this task feasible we must reduce the number of the points used. This is the motivation of the second way.

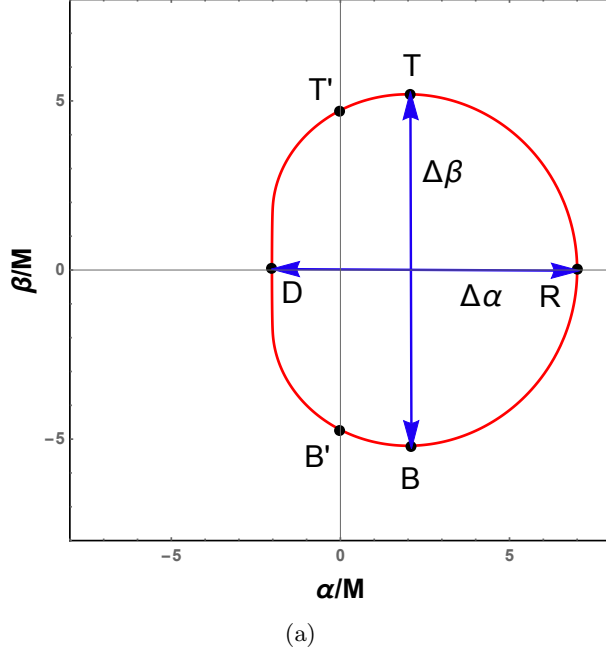


Figure 2. Sketch picture for the characteristic points of a Kerr black hole shadow. The red circle denotes the shape of the shadow with a certain spin a and viewing angle θ_0 . Characteristic points D, R, T, B are, respectively, the left, right, top, and bottom points of the shadow. Points T' and B' corresponds to $\alpha=0$. $\Delta\alpha$ and $\Delta\beta$ denote the horizontal and vertical diameters of the shadow.

For a Kerr black hole, if the inclination angle of the observer is known, one can measure any one of the observables discussed in Ref. [44] to obtain the black hole spin. However, if the angle is unknown, at least two observables must be included. We focus our attention on the characteristic points, since almost all astronomical observables are constructed from them.

For clarity, we show a schematic plot for these points in Fig. 2. Characteristic points D, R, T, B are, respectively, the left, right, top, and bottom points of the shadow. Points T' and B' correspond to $\alpha=0$. These characteristic points were examined in detail in Ref. [44]. In particular, the authors of Ref. [10] proposed two observables. One is the radius of the reference circle that passes through the points 'T', 'R', and 'B'. Although the points 'T' and 'B' are symmetric, one must use them to find the α -axis, so three points are used to obtain the radius. The other one is the distortion, which is defined by the ratio between the deformation and the radius of the reference circle. For this observable, four points 'T', 'B', 'R', and 'D' are used. After obtaining these two observables, one can get the Kerr black hole spin and the inclination angle of the observer. This method has been extended to other black hole backgrounds. So employing this method, four characteristic points on the shadow must be given in order to get a and θ_0 . However, we still want to ask whether the number of the points can be further reduced.

When we examine the property of the curvature radius R for the Kerr black hole, we find that both a and θ_0 can be determined by two symmetric characteristic points, the top point 'T' and the bottom point 'B' of the shadow. We summarize the method in the following.

Since this method closely depends on the points 'T' and 'B', let us start with them.

The points are determined by

$$(\partial_{\alpha}\beta)_{a,\theta_0} = 0. \quad (3.1)$$

Adopting the parametric forms of α and β , the condition will be reduced to

$$(\partial_{r_0}\alpha)_{a,\theta_0}^{-1} = 0, \quad (3.2)$$

or,

$$(\partial_{r_0}\beta)_{a,\theta_0} = 0. \quad (3.3)$$

The first condition (3.2) gives

$$a(M-r)^2 \sin\theta_0 = 0. \quad (3.4)$$

For $\theta_0 \neq 0$, one has $r = M$, which is smaller than the radius of the event horizon of a non-extremal black hole, and thus we turn to another condition. The second condition (3.3) gives

$$r_0^3 - 3Mr_0^2 + 3M^2r_0 - a^2M = 0, \quad (3.5)$$

or,

$$r_0^3 - 3Mr_0^2 + a^2 \cos^2\theta_0 r_0 + a^2M \cos^2\theta_0 = 0. \quad (3.6)$$

Equation (3.5) gives a real root $r_0 = M - (M^3 - Ma^2)^{\frac{1}{3}}$, which is also smaller than the radius of the event horizon, so we abandon it. Finally, by solving Eq. (3.6), we obtain

$$r_0 = M + \frac{2}{\sqrt{3}} \sqrt{3M^2 - a^2 \cos^2\theta_0} \cos\left(\frac{1}{3} \arccos\left(\frac{3\sqrt{3}M(M^2 - a^2 \cos^2\theta_0^2)}{(3M^2 - a^2 \cos^2\theta_0)^{3/2}}\right)\right). \quad (3.7)$$

Inserting this result into (α, β) , one will obtain the coordinates (α_T, β_T) of the point ‘T’. The result is complicated and we will not show the expression. But from it we can extract the vertical diameter $\Delta\beta$ of the shadow

$$\Delta\beta = 2\beta_T, \quad (3.8)$$

which is plotted as a function of a and θ_0 in Fig. 3(a). From it, we can find that $\Delta\beta$ decreases quickly when a/M approaches 1 and θ_0 approaches 0.

Furthermore, when the observer is located on the equatorial plane $\theta_0 = \frac{\pi}{2}$, we have

$$\Delta\beta = 6\sqrt{3}M, \quad (3.9)$$

which is independent of the black hole spin a . Alternatively, when $\theta_0 = 0$ and $a/M = 1$, $\Delta\beta/M = 4\sqrt{3} + 2\sqrt{2} \approx 9.6568$.

We next depict the curvature radius given in (2.15) at point ‘T’ in Fig. 3(b). For fixed θ_0 , R_T always decreases with the spin a . Interestingly, for the Schwarzschild black hole with $a/M = 0$, $R_T/M = 3\sqrt{3}$ is independent of the inclination angle θ_0 , a consequence of the spherical symmetry of the Schwarzschild black hole.

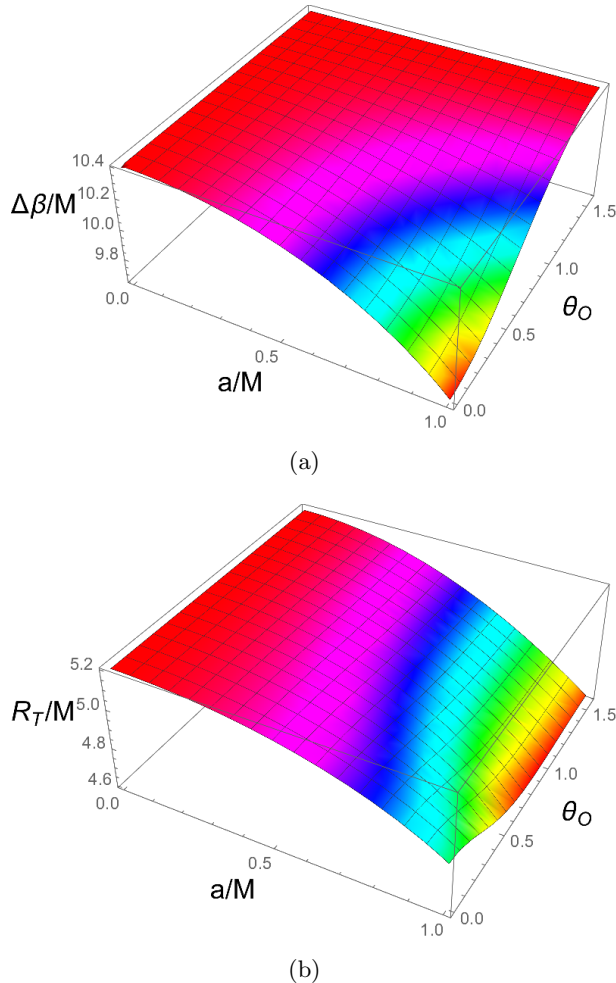


Figure 3. (a) The behavior of the vertical diameter $\Delta\beta$ of the shadow as a function of a and θ_0 . (b) The curvature radius R_T of top point ‘T’ as a function of a and θ_0 .

If we have the shape of a Kerr black hole shadow from astronomical observations, it is quite easy to obtain the α -axis, according to the \mathcal{Z}_2 symmetry of the shadow, where points ‘T’ and ‘B’ can be used. However, it is impossible to obtain the β -axis without any other information. Nevertheless, we do measure the vertical diameter $\Delta\beta$ of the shadow. So only giving the shadow, we can determine the top point ‘T’ and then get $\Delta\beta$. Moreover, the curvature radius R_T at point ‘T’ can also be obtained by the geometric method. Thus we have $\Delta\beta$ and R_T from the shape, and both depend on the black hole spin a and the inclination angle θ_0 . Next, we can solve a and θ_0 from these two observables. For an example, we plot the contour lines of $\Delta\beta$ and R_T in Fig. 4 in the θ_0 - a plane with $\Delta\beta/M = 9.70, 9.76, 9.82, 9.88, 9.94, 10.00, 10.06, 10.12, 10.18, 10.24, 10.3, 10.36, 10.39$ from bottom right to top left and $R_T/M = 4.65, 4.695, 4.74, 4.785, 4.83, 4.875, 4.92, 4.965, 5.01, 5.055, 5.1, 5.145, 5.19$ from right to left. The red solid lines are for $\Delta\beta$ and blue dashed lines for R_T . From this figure, we can directly read out the black hole spin a and the location of the observer θ_0 with given β_T and R_T .

A few comments are worth making at this point about this method. i) It uses only two symmetric characteristic points to simultaneously determine both a and θ_0 . ii) It de-

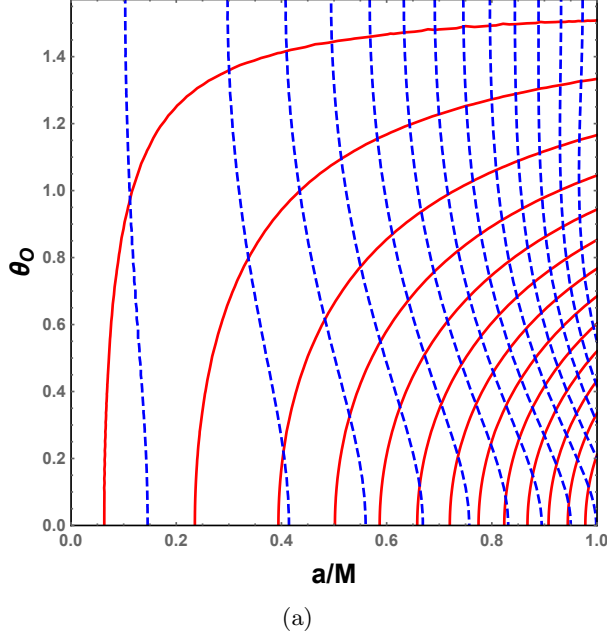


Figure 4. Contour lines of $\Delta\beta$ and R_T . The red solid lines are for $\Delta\beta/M = 9.70, 9.76, 9.82, 9.88, 9.94, 10.00, 10.06, 10.12, 10.18, 10.24, 10.3, 10.36, 10.39$ from bottom right to top left. The blue dashed lines are for $R_T/M = 4.65, 4.695, 4.74, 4.785, 4.83, 4.875, 4.92, 4.965, 5.01, 5.055, 5.1, 5.145, 5.19$ from right to left.

pend only on the intrinsic properties of the shape of the shadow, and is independent of the coordinates. iii) Although more black hole parameters are included when considering other non-Kerr black holes, we believe that by making use of the curvature radius, the number of the points that must be used will be greatly reduced.

3.2 Approach II

From approach I, we see that the parameters a and θ_0 can be both determined by measuring β_T and the curvature radius at point ‘T’. Can we determine a and θ_0 using only the curvature radius? The answer is ‘yes’ as we shall now demonstrate.

We have previously shown [39] that when excluding the \mathcal{Z}_2 symmetry, there exists one maximum and one minimum of the curvature R_T for fixed a and θ_0 . Combining these two curvature radii, we show that a and θ_0 can be uniquely determined [39]. However, although the maximum one is at point ‘D’, the minimum is uncertain. But we can replace the point of minimum curvature with other characteristic points, for example point ‘R’ or ‘D’. Thus, we need only measure the curvature of any two points of ‘T’, ‘R’, and ‘D’ to obtain a and θ_0 . According to this idea, by measuring the curvature for any two points without symmetry on the boundary of the black hole shadow, we can obtain a and θ_0 . Nevertheless, one should keep in mind that, given a shape of the shadow, we must first use points ‘T’ and ‘B’ to find out the α -axis. So in this approach, at least, three points must be included in. Thus comparing with approach I, this approach uses more points. Hence, it also provides us a novel approach for using the curvature radius.

After obtaining the curvature radii of points ‘D’, ‘T’, and ‘R’, we depict in Fig. 5 the respective contour lines R_D , R_T , and R_R in θ_0 - a plane by using two of them. Each point in

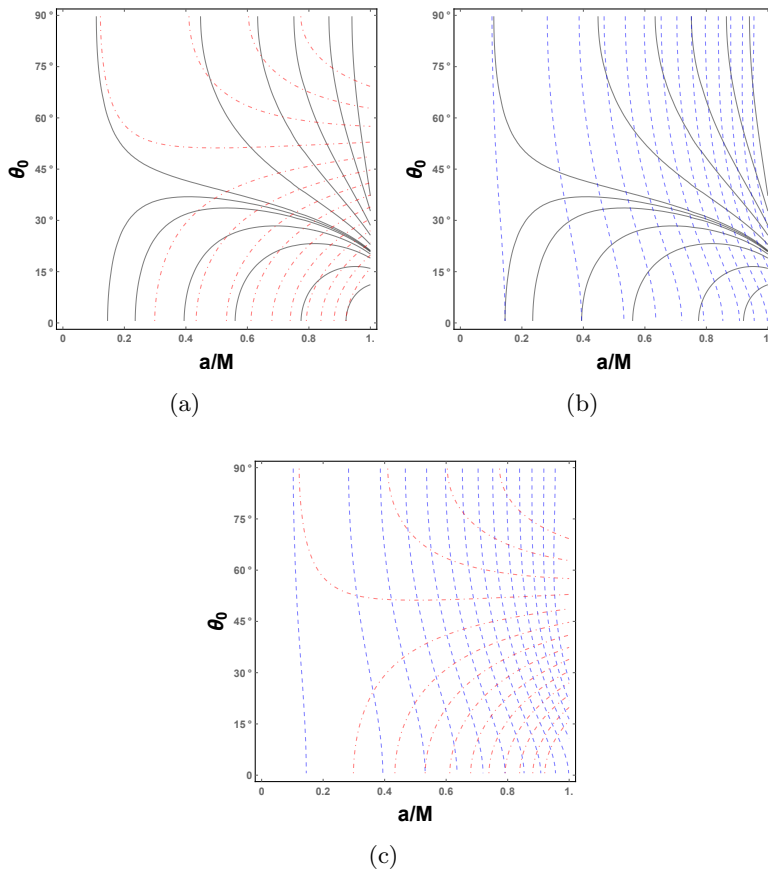


Figure 5. Contour lines of R_D , R_T , and R_R in θ_0 - a plane. The black solid lines are for $R_D/M=4.9, 5, 5.1, 5.15, 5.18, 5.19, 5.2, 5.3, 5.5, 5.8, 6.5, 8, 10, 14$ from bottom to top. The red dot dashed lines are for $R_R/M=4.9, 4.93, 4.96, 4.99, 5.02, 5.05, 5.08, 5.11, 5.14, 5.17, 5.2, 5.23, 5.26, 5.29$ from bottom to top. The blue dashed lines are for $R_T/M= 4.67, 4.71, 4.75, 4.79, 4.83, 4.87, 4.91, 4.95, 4.99, 5.03, 5.07, 5.11, 5.15, 5.19$ from right to left. (a) Contour lines of R_D and R_R . (b) Contour lines of R_D and R_T . (c) Contour lines of R_R and R_T .

these figures is characterized by a pair values of (a, θ_0) . So if we know any two of R_D , R_T , and R_R , we can read out (a, θ_0) immediately from the figures.

3.3 Approach III

In the above two approaches, we showed how to use the curvature radius of different characteristic points to determine the black hole spin and the inclination angle. However in practice their variation as a and θ_0 change is very small. For a comparison, we list in Table 1 their values for $a=0$ and 1 for an equatorial observer. It is clear that the curvature radii R_T and R_R experience small changes. The vertical diameter $\Delta\beta$ keeps the same value, while the horizontal diameter $\Delta\alpha$ and R_D significantly change.

Consequently using $\Delta\alpha$ and R_D may yield higher accuracy in determining a and θ_0 . Keeping this in mind, we show the contour lines of $\Delta\alpha$ and R_D in Fig. 6 with $\Delta\alpha/M=9.09, 9.29, 9.39, 9.49, 9.59, 9.69, 9.79, 9.89, 9.99, 10.09, 10.19, 10.29, 10.36, 10.39$, and $R_D/M=4.9, 5, 5.1, 5.15, 5.18, 5.19, 5.2, 5.3, 5.5, 5.8, 6.5, 8, 10, 14$. Similarly, each point on the figure is characterized by a pair values of (a, θ_0) and a pair values of $(\Delta\alpha, R_D)$. Hence the values

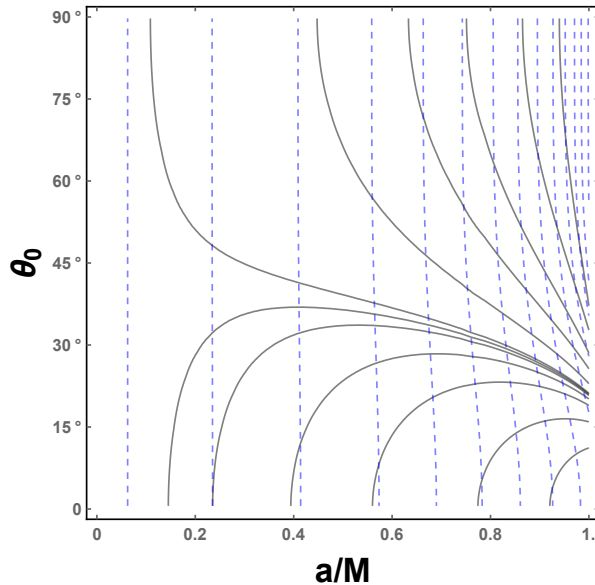


Figure 6. Contour lines of $\Delta\alpha$ and R_D . The blue dashed lines are for $\Delta\alpha/M=9.09, 9.29, 9.39, 9.49, 9.59, 9.69, 9.79, 9.89, 9.99, 10.09, 10.19, 10.29, 10.36, 10.39$ from right to left. The black solid lines are for $R_D/M=4.9, 5, 5.1, 5.15, 5.18, 5.19, 5.2, 5.3, 5.5, 5.8, 6.5, 8, 10, 14$ from bottom to top.

of the parameters a and θ_0 can be easily read out by giving $\Delta\alpha$ and R_D . Moreover, from Fig. 6, we can find that, for fixed spin a , the horizontal diameter $\Delta\alpha$ almost keeps the same constant for different θ_0 .

	R_D/M	R_T/M	R_R/M	$\Delta\alpha/M$	$\Delta\beta/M$
$a/M = 0$	$3\sqrt{3}$	$3\sqrt{3}$	$3\sqrt{3}$	$6\sqrt{3}$	$6\sqrt{3}$
$a/M = 1$	∞	$\frac{8}{\sqrt{3}}$	$\frac{16}{3}$	9	$6\sqrt{3}$
δ	∞	0.5774	0.1372	1.3923	0

Table 1. Values for the curvature radii at points ‘D’, ‘T’, ‘R’, the horizontal diameter $\Delta\alpha$, and the vertical diameter $\Delta\beta$ of the black hole shadow seen by an equatorial observer with $\theta_0 = \frac{\pi}{2}$. The parameter δ denotes the change of these quantities between the Schwarzschild black hole $a/M = 0$ and the extremal Kerr black hole $a/M = 1$.

4 Application to M87*

A couple of days ago EHT showcased the first image of a black hole. Specifically they obtained the image of the supermassive black hole located in the centre of the massive elliptical galaxy M87 [1, 2]. This provides us with a new observational window to test strong gravity near the horizon of a black hole. Here we calculate the diameters and curvature radii for the black hole shadow of M87*. With increased observational precision we expect this can be helpful in testing the fine structure of spacetime near a supermassive black hole.

Taking the values of the parameters of the M87* from EHT observations [3], i.e., the distance between us and M87* is $D = 16.8$ Mpc and its mass is $M = 6.5 \times 10^9 M_\odot$, we can

calculate the gravitational radius [3]

$$\theta_g = \frac{GM}{c^2 D} \approx 3.8 \mu\text{as} \quad . \quad (4.1)$$

Since the approaching jet and the line of sight is 16° [48], we only focus our attention on the viewing angle θ_0 around 16° . Moreover, adopting the Standard and Normal Evolution (SANE) and Magnetically Arrested Disk (MAD) models, one can find from the rejection table of [2] that the black hole spin $|a|=0.5$ and 0.94 can pass these different constraints. Thus we consider values of a within this range in our calculation.

We show the horizontal and vertical diameters of the black hole shadow cast by M87* in Fig. 7 with varying the viewing angle $\theta_0=10^\circ, 13^\circ, 16^\circ, 19^\circ, 22^\circ$, respectively. For fixed θ_0 , both the diameters $\Delta\alpha$ and $\Delta\beta$ decrease with the black hole spin. For fixed black hole spin a , $\Delta\alpha$ decreases whereas $\Delta\beta$ increases with increasing θ_0 . At $a = 0.5$, both $\Delta\alpha$ and $\Delta\beta$ are near $38.9 \mu\text{as}$. When a increases to 0.94 , the vertical diameter $\Delta\beta$ is about $37.3 \mu\text{as}$. The horizontal diameter $\Delta\alpha$ can even approach $37 \mu\text{as}$. Thus the shape of the shadow will be increasingly deformed for high spin. Moreover, for low spin, $\Delta\alpha$ and $\Delta\beta$ are almost independent of the viewing angle θ_0 .

The curvature radii at points ‘D’, ‘T’, ‘R’ are each plotted against the black hole spin in Fig. 8 for $\theta_0=10^\circ, 13^\circ, 16^\circ, 19^\circ, 22^\circ$. For small viewing angle θ_0 , R_D decreases with the black hole spin. However for θ_0 larger than 13° , e.g., $\theta_0 = 22^\circ$, R_D first decreases from about $19.6 \mu\text{as}$ to $19.3 \mu\text{as}$ and then increases to $19.4 \mu\text{as}$ with increasing a . Thus, if $\theta_0 > 13^\circ$ we cannot determine the black hole spin even if R_D is known, unless some other conditions are considered. Meanwhile, when a varies from 0.5 to 0.94 , R_T decreases from $19.4 \mu\text{as}$ to $18.2 \mu\text{as}$, and R_R decreases from $19.5 \mu\text{as}$ to $18.7 \mu\text{as}$.

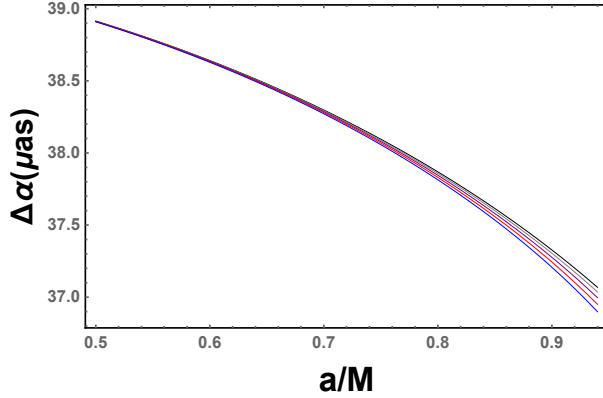
a/M	0.5	0.6	0.7	0.8	0.9	0.94
$\Delta\alpha(\mu\text{as})$	38.91	38.64	38.29	37.85	37.28	37.00
$\Delta\beta(\mu\text{as})$	38.96	38.71	38.40	38.03	37.56	37.34
$R_D(\mu\text{as})$	19.51	19.40	19.28	19.14	19.01	18.97
$R_T(\mu\text{as})$	19.50	19.39	19.25	19.08	18.87	18.78
$R_R(\mu\text{as})$	19.43	19.28	19.09	18.84	18.51	18.35

Table 2. Angular size of the quantities for the shadow cast by M87* with viewing angle $\theta_0 = 16^\circ$.

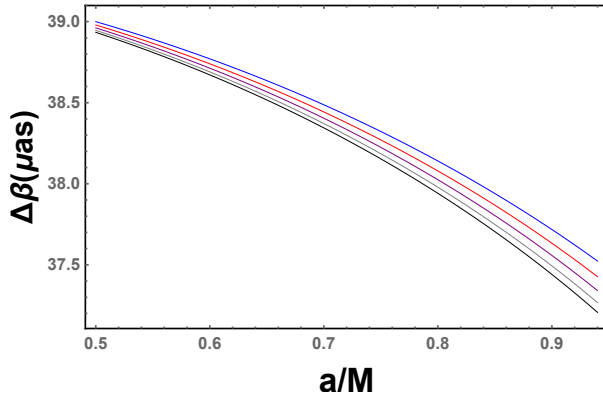
For comparison, we list the values of these quantities $\Delta\alpha$, $\Delta\beta$, R_D , R_T , and R_R in Table 2 when $\theta_0 = 16^\circ$ is fixed. For two small values of the spin, the differences between them are very tiny. However, for two high spins $a/M=0.7$ and 0.94 , the differences of $\Delta\alpha$, $\Delta\beta$, R_D , R_T , and R_R between them are, respectively, about 1.3 , 1.1 , 0.3 , 0.5 , and $0.7 \mu\text{as}$. Thus, when the precision of EHT is improved to around $1 \mu\text{as}$ comparing with current resolution $5 \mu\text{as}$ in the final reconstructed images, the black hole spin can be well determined in high spin case.

5 Conclusions and discussions

In this paper, we mainly considered the application of the curvature radius we previously proposed [39]. Based on the characteristic points and making use of the curvature radius, we have put forward three novel approaches to determine the spin of the Kerr black hole and the inclination angle of the observer.



(a)



(b)

Figure 7. The horizontal diameter $\Delta\alpha$ and the vertical diameter $\Delta\beta$ of the shadow cast by M87*. (a) $\Delta\alpha$ vs a . The viewing angle $\theta_0=10^\circ, 13^\circ, 16^\circ, 19^\circ, 22^\circ$ from top to bottom. (b) $\Delta\beta$ vs a . The viewing angle $\theta_0=10^\circ, 13^\circ, 16^\circ, 19^\circ, 22^\circ$ from bottom to top.

The first approach makes use of only two symmetric characteristic points, ‘T’ and ‘B’ to determine a and θ_0 . This is the fewest number of points required, and is in contrast to previous approaches [10] requiring four characteristic points, ‘D’, ‘R’, ‘T’, and ‘B’.

In the second approach we obtain a and θ_0 by only finding the curvature radii of these characteristic points.

The third approach employs the horizontal diameter $\Delta\alpha$ and the curvature radius R_D of point ‘D’ to determine a and θ_0 . The former quantities have the most sensitive dependence on the latter and so may provide a more accurate way to determine the spin and the viewing angle.

The three approaches above can provide an analytic result from a rather small amount of information. In astronomical observations [1, 2, 4, 5] shadows are expected to be obtained with uncertainty, and a fit to the observed image might be performed to obtain the black hole parameters using Eqs. (2.11) and (2.12).

Although our results are mainly for the Kerr black hole, it is easy to extend to other black hole backgrounds, where perhaps, more black hole parameters are present. Consequently more characteristic points will have to be considered to fix the black hole parameters and the inclination angle of the observer. Though it remains to be demonstrated, we believe that

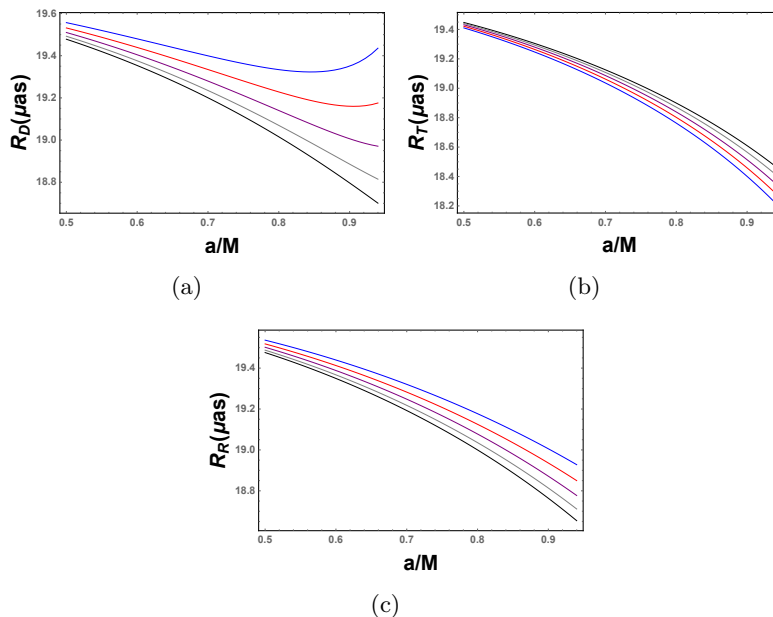


Figure 8. Curvature radii at points ‘D’, ‘T’, ‘R’ for the shadow cast by M87*. (a) R_D vs a . $\theta_0=10^\circ, 13^\circ, 16^\circ, 19^\circ, 22^\circ$ from bottom to top. (b) R_T vs a . $\theta_0=10^\circ, 13^\circ, 16^\circ, 19^\circ, 22^\circ$ from top to bottom. (c) R_R vs a . $\theta_0=10^\circ, 13^\circ, 16^\circ, 19^\circ, 22^\circ$ from bottom to top.

our approaches will still be applicable to determine the various black hole parameters.

Finally, we applied our study of the curvature radius to the supermassive black hole M87*. We computed the angular size for the horizontal diameter $\Delta\alpha$, the vertical diameter $\Delta\beta$, and curvature radii R_D , R_T , R_R . When the black hole spin increases from 0.5 to 0.94, both $\Delta\alpha$ and $\Delta\beta$ are about $38.9 \mu\text{as}$, and then approach $37.0 \mu\text{as}$ and $37.3 \mu\text{as}$, respectively. For $a/M = 0.5$, the curvature radii R_D , R_T , and R_R are all about $19.5 \mu\text{as}$, and then go to $19.0 \mu\text{as}$, $18.8 \mu\text{as}$, and $18.4 \mu\text{as}$, respectively. With improved observational resolution and reconstruction, we expect that the nature of M87* will be well determined through its shadow.

In closing, by focussing on the local properties of the shadow at several characteristic points, we have shown that information about the black hole can be completely determined from these local properties. However for an astronomical applications, this requires obtaining a sufficiently high resolution image of the shadow edge. Although the current resolution of the EHT cannot achieve this, we expect that our method will be applicable in the (near) future once high-resolution shadow images become available. In contrast to integrated approaches that combine information over the entire shadow edge, our method provides a useful alternative for extracting information from the shadows of black holes. Furthermore, there exist bright lensing rings around black hole shadows, and these are more easily observed. The innermost one is very close to the black hole edge, and it can be naturally treated as if it were the black hole edge, in which case our approach can be easily used. Moreover, we can directly apply our concept of the curvature radius, since the light ring is also one dimensional, and then extract information about the black hole.

In summary, the curvature radius is a novel concept, one that we expect will prove useful from both theoretical and observational perspectives in understanding the strong gravitational effects of black holes.

Acknowledgements

This work was supported by the National Natural Science Foundation of China (Grants Nos. 11675064, 11875151, 11522541, and U1738132) and the Natural Sciences and Engineering Research Council of Canada. S.-W. Wei was also supported by the Chinese Scholarship Council (CSC) Scholarship (201806185016) to visit the University of Waterloo.

References

- [1] The Event Horizon Telescope Collaboration, *First M87 Event Horizon Telescope Results. I. The Shadow of the Supermassive Black Hole*, *Astrophys. J. Lett.* **875**, L1 (2019).
- [2] The Event Horizon Telescope Collaboration, *First M87 Event Horizon Telescope Results. V. Physical Origin of the Asymmetric Ring*, *Astrophys. J. Lett.* **875**, L5 (2019).
- [3] The Event Horizon Telescope Collaboration, *First M87 Event Horizon Telescope Results. VI. The Shadow and Mass of the Central Black Hole*, *Astrophys. J. Lett.* **875**, L6 (2019).
- [4] A. M. Hughes, A. Beasley, and C. Carilli, *Next Generation Very Large Array: Centimeter Radio Astronomy in the 2020s*, IAU General Assembly, **22**, 2255106 (2015).
- [5] G. H. Sanders, *The Thirty Meter Telescope (TMT): An International Observatory*, *Journal of Astrophysics and Astronomy*, **34**, 81 (2013).
- [6] J. L. Synge, *The escape of photons from gravitationally intense stars*, *MNRAS*, **131**, 463 (1966).
- [7] J. P. Luminet, *Image of a spherical black hole with thin accretion disk*, *A. A.*, **75**, 228 (1979).
- [8] J. M. Bardeen, *Timelike and null geodesics in the Kerr metric*, *Les Astres Occlus*, (1973).
- [9] S. Chandrasekhar, *The Mathematical Theory of Black Holes*, Oxford University Press, New York, (1992).
- [10] K. Hioki and K. I. Maeda, *Measurement of the Kerr Spin Parameter by Observation of a Compact Object's Shadow*, *Phys. Rev. D* **80**, 024042 (2009), [arXiv:0904.3575 [astro-ph.HE]].
- [11] T. Johannsen, *Photon rings around Kerr and Kerr-like black holes*, *Astrophys. J.* **777**, 170 (2013), [arXiv:1501.02814 [astro-ph.HE]].
- [12] M. Ghasemi-Nodehi, Z.-L. Li, and C. Bambi, *Shadows of CPR black holes and tests of the Kerr metric*, *Eur. Phys. J. C* **75**, 315 (2015), [arXiv:1506.02627 [gr-qc]].
- [13] C. Bambi and K. Freese, *Apparent shape of super-spinning black holes*, *Phys. Rev. D* **79**, 043002 (2009), [arXiv:0812.1328 [astro-ph]].
- [14] L. Amarilla, E. F. Eiroa, and G. Giribet, *Null geodesics and shadow of a rotating black hole in extended Chern-Simons modified gravity*, *Phys. Rev. D* **81**, 124045 (2010), [arXiv:1005.0607 [gr-qc]].
- [15] Z. Stuchlik and J. Schee, *Appearance of Keplerian discs orbiting Kerr superspinars*, *Class. Quant. Grav.* **27**, 215017 (2010), [arXiv:1101.3569 [gr-qc]].
- [16] L. Amarilla and E. F. Eiroa, *Shadow of a Kaluza-Klein rotating dilaton black hole*, *Phys. Rev. D* **87**, 044057 (2013), [arXiv:1301.0532 [gr-qc]].
- [17] P. G. Nedkova, V. K. Tinchev, and S. S. Yazadjiev, *The shadow of a rotating traversable wormhole*, *Phys. Rev. D* **88**, 124019, (2013) [arXiv:1307.7647 [gr-qc]].
- [18] S.-W. Wei and Y.-X. Liu, *Observing the shadow of Einstein-Maxwell-Dilaton-Axion black hole*, *JCAP* **1311**, 063 (2013), [arXiv:1311.4251 [gr-qc]].
- [19] N. Tsukamoto, Z.-L. Li, and C. Bambi, *Constraining the spin and the deformation parameters from the black hole shadow*, *JCAP* **1406**, 043 (2014), [arXiv:1403.0371 [gr-qc]].

- [20] C. Bambi and N. Yoshida, *Shape and position of the shadow in the $\delta=2$ Tomimatsu-Sato space-time*, Class. Quant. Grav. **27**, 205006 (2010), [arXiv:1004.3149 [gr-qc]].
- [21] F. Atamurotov, A. Abdujabbarov, and B. Ahmedov, *Shadow of rotating non-Kerr black hole*, Phys. Rev. D **88**, 064004 (2013).
- [22] S. Abdolrahimi, R. B. Mann, and C. Tzounis, *Distorted local shadows*, Phys. Rev. D **91**, 084052 (2015), [arXiv:1502.00073 [gr-qc]].
- [23] S.-W. Wei, P. Cheng, Y. Zhong, and X.-N. Zhou, *Shadow of noncommutative geometry inspired black hole*, JCAP **1508**, 004 (2015), [arXiv:1501.06298 [gr-qc]].
- [24] F. Atamurotov, B. Ahmedov, and A. Abdujabbarov, *Optical properties of black hole in the presence of plasma: shadow*, Phys. Rev. D **92**, 084005 (2015), [arXiv:1507.08131 [gr-qc]].
- [25] A. Abdujabbarov, M. Amir, B. Ahmedov, and S. G. Ghosh, *Shadow of rotating regular black holes*, Phys. Rev. D **93**, 104004 (2016), [arXiv:1604.03809 [gr-qc]].
- [26] M.-Z. Wang, S.-B. Chen, and J.-L. Jing, *Shadow casted by a Konoplya-Zhidenko rotating non-Kerr black hole*, JCAP **1710**, 051 (2017), [arXiv:1707.09451 [gr-qc]].
- [27] M. Amir, B. P. Singh, and S. G. Ghosh, *Shadows of rotating five-dimensional charged EMCS black holes*, Eur. Phys. J. C **78**, 399 (2018), [arXiv:1707.09521 [gr-qc]].
- [28] N. Tsukamoto, *Black hole shadow in an asymptotically-flat, stationary, and axisymmetric spacetime: The Kerr-Newman and rotating regular black holes*, Phys. Rev. D **97**, 064021 (2018), [arXiv:1708.07427 [gr-qc]].
- [29] M.-Z. Wang, S.-B. Chen, and J.-L. Jing, *Shadows of Bonnor black dihole by chaotic lensing*, Phys. Rev. D **97**, 064029 (2018), [arXiv:1710.07172 [gr-qc]].
- [30] R. Shaikh, *Shadows of rotating wormholes*, Phys. Rev. D **98**, 024044 (2018), [arXiv:1803.11422 [gr-qc]].
- [31] X. Hou, Z.-Y. Xu, M. Zhou, and J.-C. Wang, *Black hole shadow of Sgr A* in dark matter halo*, JCAP **1807**, 015 (2018), [arXiv:1804.08110 [gr-qc]].
- [32] P. V. P. Cunha, C. A. R. Herdeiro, E. Radu, and H. F. Runarsson, *Shadows of Kerr black holes with scalar hair*, Phys. Rev. Lett. **115**, 211102 (2015), [arXiv:1509.00021 [gr-qc]].
- [33] P. V. P. Cunha, C. A. R. Herdeiro, and E. Radu, *Fundamental photon orbits: black hole shadows and spacetime instabilities*, Phys. Rev. D **96**, 024039 (2017), [arXiv:1705.05461 [gr-qc]].
- [34] P. V. P. Cunha and C. A. R. Herdeiro, *Shadows and strong gravitational lensing: a brief review*, Gen. Rel. Grav. **50**, 42 (2018), [arXiv:1801.00860 [gr-qc]].
- [35] O. Yu. Tsupko, *Analytical calculation of black hole spin using deformation of the shadow*, Phys. Rev. D **95**, 104058 (2017), [arXiv:1702.04005 [gr-qc]].
- [36] V. Perlick, O. Yu. Tsupko, and G. S. Bisnovatyi-Kogan, *Black hole shadow in an expanding universe with a cosmological constant*, Phys. Rev. D **97**, 104062 (2018), [arXiv:1804.04898 [gr-qc]].
- [37] R. Shaikh, P. Kocherlakota, R. Narayan, and P. S. Joshi, *Shadows of spherically symmetric black holes and naked singularities*, Mon. Not. Roy. Astron. Soc. **482**, 52 (2019), [arXiv:1802.08060 [astro-ph.HE]].
- [38] H.-M. Wang, Y.-M. Xu, and S.-W. Wei, *Shadows of Kerr-like black holes in a modified gravity theory*, JCAP **1903**, 046 (2019), [arXiv:1810.12767 [gr-qc]].
- [39] S.-W. Wei, Y.-X. Liu, and R. B. Mann, *Intrinsic curvature and topology of shadow in Kerr spacetime*, Phys. Rev. D **99**, 041303(R) (2019), [arXiv:1811.00047 [gr-qc]].

- [40] Z. Younsi, A. Zhidenko, L. Rezzolla, R. Konoplya, and Y. Mizuno, *New method for shadow calculations: Application to parametrized axisymmetric black holes*, Phys. Rev. D **94**, 084025 (2016) [arXiv:1607.05767 [gr-qc]].
- [41] A. K. Mishra, S. Chakraborty, and S. Sarkar, *Understanding photon sphere and black hole shadow in dynamically evolving spacetimes*, [arXiv:1903.06376 [gr-qc]].
- [42] A. B. Abdikamalov, A. A. Abdujabbarov, D. Malafarina, C. Bambi, and B. Ahmedov, *A black hole mimicker hiding in the shadow: Optical properties of the γ metric*, [arXiv:1904.06207 [gr-qc]].
- [43] A. A. Abdujabbarov, L. Rezzolla, and B. J. Ahmedov, *A coordinate-independent characterization of a black hole shadow*, Mon. Not. Roy. Astron. Soc. **454**, 2423 (2015), [arXiv:1503.09054 [gr-qc]].
- [44] S.-W. Wei and Y.-X. Liu, *Parametric study of Kerr black hole shadow: analytical and exact calculations*, in preparation, (2019).
- [45] K. Yano, *Some remarks on tensor fields and curvature*, Ann. Math. **55**, 328 (1952).
- [46] R. Penrose, *Naked singularities*, Ann. N. Y. Acad. Sci. **224**, 125 (1973).
- [47] P. J. Young, *Capture of particles from plunge orbits by a black hole*, Phys. Rev. D **14**, 3281 (1976).
- [48] R. C. Walker, P. E. Hardee, F. B. Davies, C. Ly, and W. Junor, *The Structure and Dynamics of the Sub-parsec Scale Jet in M87 Based on 50 VLBA Observations Over 17 Years at 43 GHz*, Astrophys. J. **855**, 128 (2018), [arXiv:1802.06166 [astro-ph.HE]].